# Figure S1 (related to main Figure 1)

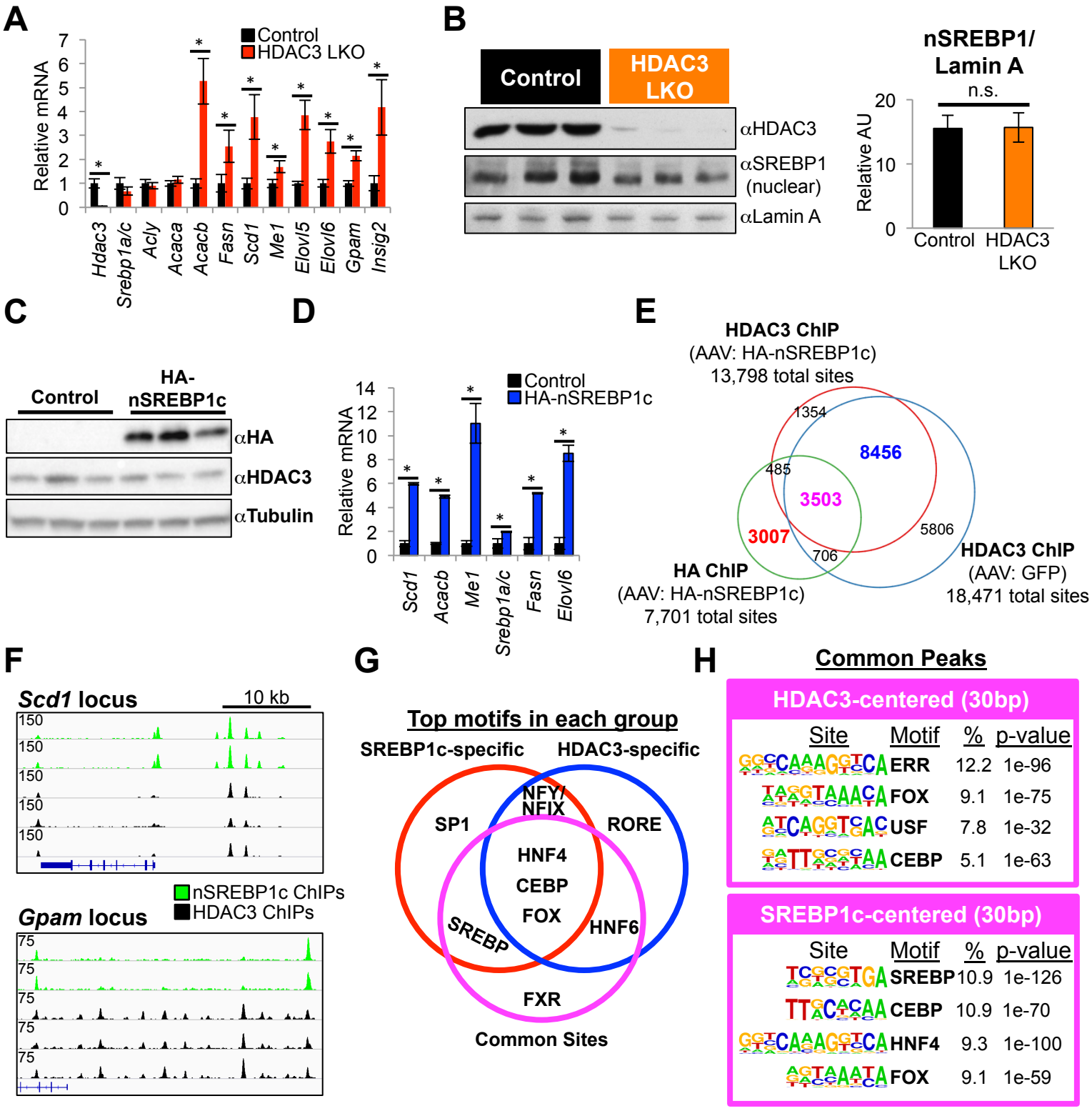


**Figure S1 (related to main Figure 1). HDAC3 and SREBP1c independently bind near lipogenic genes to regulate their transcription.** (**A**) RT-qPCR analysis of lipid metabolic gene expression in livers. *n* = 3 mice per group. Mice were sacrificed 15 days post AAV8 injections. (**B**) Western blot analysis and quantification of nuclear SREBP1 levels in livers of indicated mice. Control, AAV8:GFP injected; HDAC3 LKO, AAV8:Cre injected. (**C**) Western blot analysis of whole liver lysates from C57Bl/6 mice injected with either AAV8:GFP (Control) or AAV8:HA-nSREBP1c (HA-nSREBP1c). (**D**) RT-qPCR analysis of lipid metabolic gene expression in livers from mice described in **C**. *n* = 3 mice per group. (**E**) Venn diagram of high-confidence peaks identified in the three experimental conditions. Common peaks (purple), HDAC3-specific peaks (blue), and SREBP1c peaks (red), were used in the analysis for main Figure 1. (**F**) Genome browser view of HDAC3 and HA-nSREBP1c peaks at lipogenic gene loci. Biological replicates are shown. For HDAC3 ChIPs, mice were injected with AAV8:GFP. (**G**) Venn diagram of enriched motifs for each assigned group. (**H**) *De novo* motif analysis of common peaks centered at each factor and searched +/- 15 bp from each center.

All error bars, s.e.m. Significance was determined by two-tailed Student's *t* test (*$P < 0.05$ for comparisons between experimental and control mice).

# Figure S2 (related to main Figure 2)

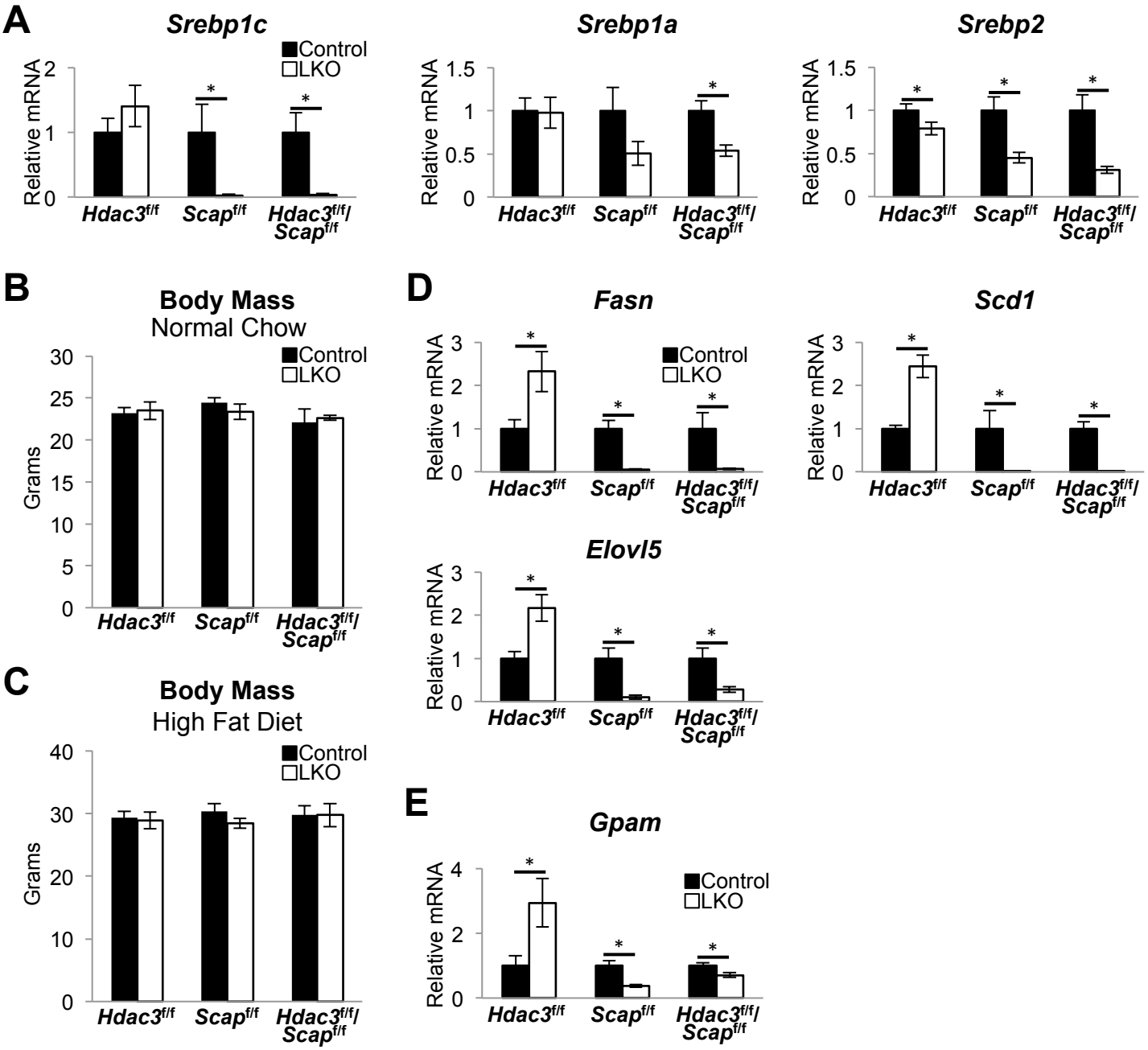


**Figure S2 (related to main Figure 2). HDAC3 partially suppresses fatty liver formation in SCAP depleted livers.** (**A**) RT-qPCR analysis of *Srebp* isoforms in livers from mice sacrificed 10 days post AAV8 injection. Control, AAV8:GFP injected; LKO, AAV8:Cre injected. $n = 4$ to 5 mice per group. (**B**) Body mass of mice described in **A**. (**C**) Body mass of mice fed a high-fat diet for 8 weeks total (injected with AAV8 at 6 weeks). Indicated floxed mice were injected with AAV8:GFP (Control) or AAV8:Cre (LKO). $n = 4$ to 5 mice per group. (**D**) RT-qPCR analysis of lipogenic gene expression in livers from HFD fed mice described in **C**. (**E**) RT-qPCR analysis of *Gpam* gene expression in livers from HFD fed mice described in **C**.

All error bars, s.e.m. Significance was determined by two-tailed Student's *t* test (*$P < 0.05$ for comparisons between experimental and control mice).

# Figure S3 (related to main Figure 3)

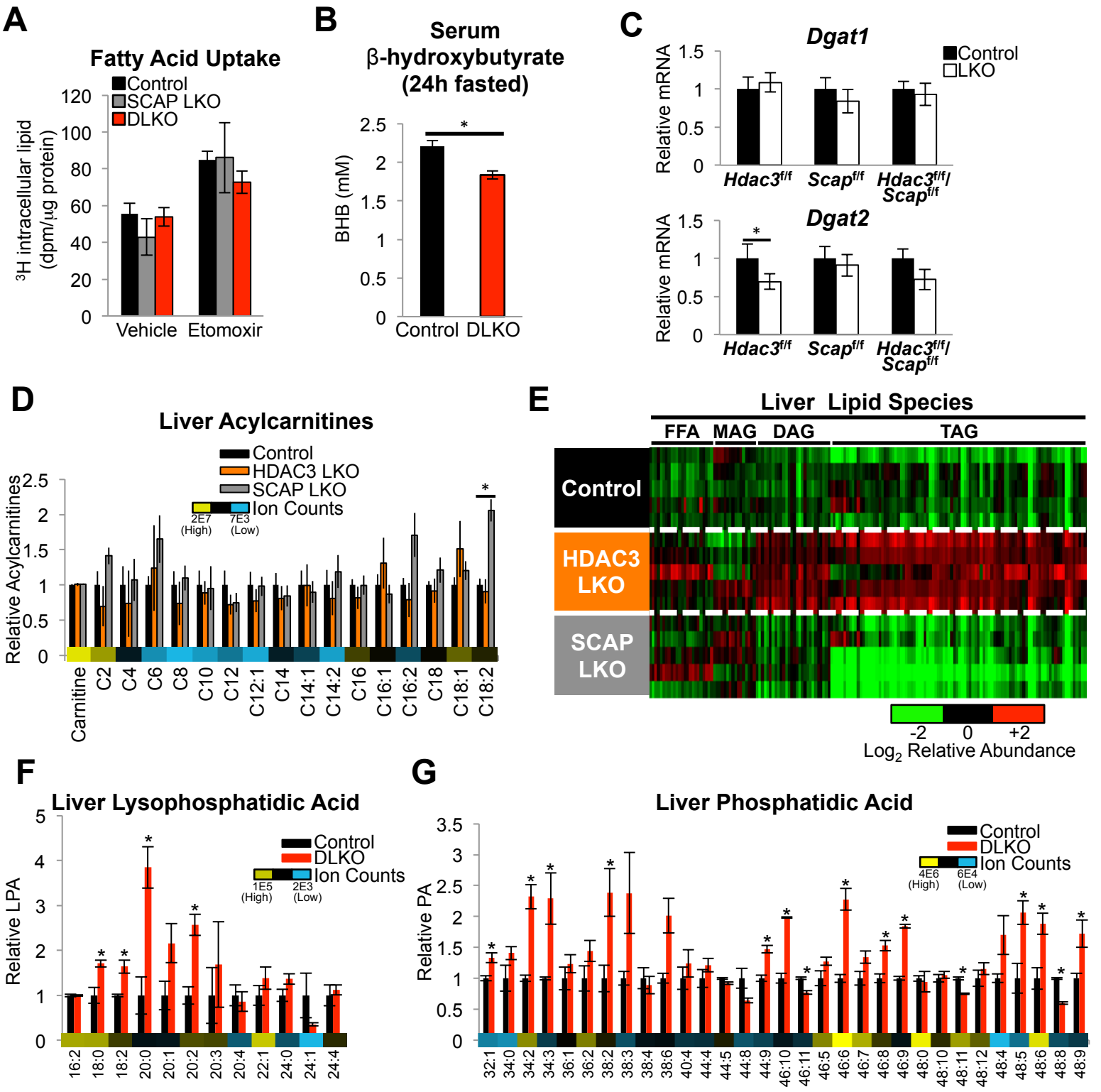


**Figure S3 (related to main Figure 3). Decreased fatty acid oxidation and accumulation of lipid intermediates in livers lacking HDAC3 and SCAP.** (**A**) Fatty acid uptake measured in the same primary hepatocytes as in main Figure 3A. $^{3}$H-labelled intracellular lipids was extracted and measured by scintillation counting. dpm, disintegrations per minute. Vehicle (water) treated, $n = 4$ wells (combined from 2 mice) per group. Etomoxir treated, $n = 3$ to 4 wells (combined from 2 mice) per group. Significance was determined by one-way ANOVA with Tukey's correction (*$P < 0.05$). (**B**) Fasting serum ketone body concentrations. $n = 4$ mice per group. *$P < 0.05$, two-tailed Student's $t$ test. (**C**) RT-qPCR analysis of *Dgat* expression in livers. $n = 4$ to 5 mice per group. *$P < 0.05$, two-tailed Student's $t$ test. (**D** and **E**) Hepatic levels of acylcarnitines (D) and other lipid species (E) in Control, HDAC3 LKO and SCAP LKO mice as measured by liquid chromatography mass spectrometry. Average ion counts of each metabolite across all conditions are shown in (D). $n = 5$ mice per group. Significance was determined one-way ANOVA followed by FDR correction (*$P < 0.05$). Ion counts are available in Table S2. (**F** and **G**) Hepatic levels of indicated lipids as measured by liquid chromatography mass spectrometry. Average ion counts of each metabolite across all conditions are shown. $n = 4$ mice per group. Significance was determined by Student's two-tailed $t$ test followed by FDR correction (*P <0.05). Ion counts are available in Table S1.

All error bars, s.e.m.

# Figure S4 (related to main Figure 4)

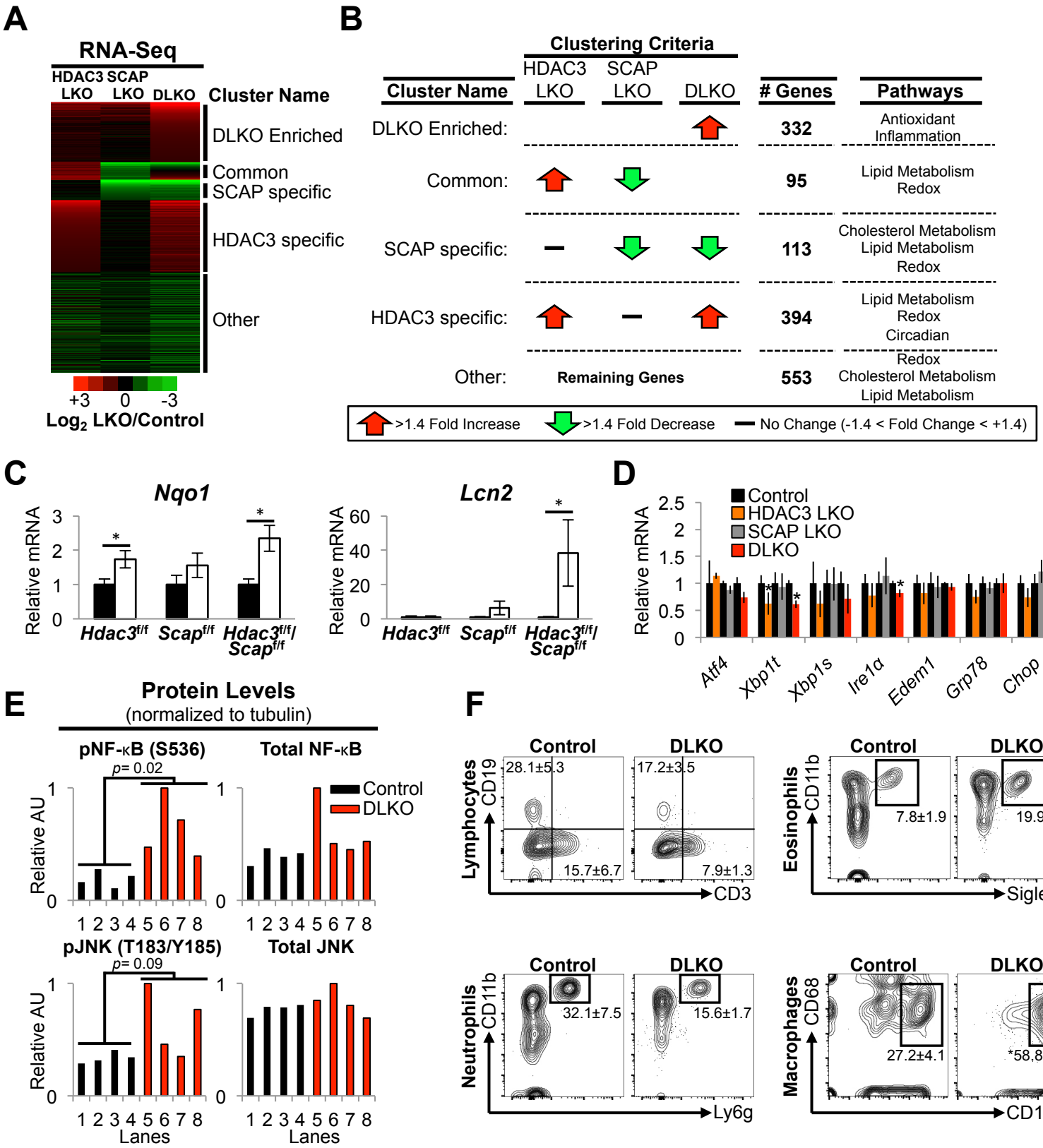


**Figure S4 (related to main Figure 4). Lack of HDAC3 and SCAP causes hepatic lipotoxicity, oxidative stress, and inflammation.** (**A**) Heat map of RNA-seq data from livers of indicated mice. (**B**) Clustering criteria for the RNA-seq data. Differentially expressed transcripts with an FDR <0.1 in at least once condition were used. The comparison groups were between control ($n$ = 6) and HDAC3 LKO mice ($n$ = 4), SCAP LKO mice ($n$ = 4), or DLKO mice ($n$ = 3). Processed RNA-seq data are available in Table S3. (**C** and **D**) RT-qPCR analysis of NF-kB target genes (C) and ER stress genes (D) in livers. $n$ = 4 to 5 mice per group. *$P$ < 0.05, two-tailed Student's $t$ test. Error bars, s.e.m. (**E**) Quantification of western blots from main Figure 4E. Significance was determined by two-tailed Student's $t$ test. (**F**) Flow cytometric analysis of liver immune cells from Control or DLKO mice. Numbers adjacent to outlined areas indicate percentage of cells in each gate (average +/- s.e.m). Lymphocytes gated on CD45+ cells. Myloid cells gated on CD45+, CD3-, CD19-. Significance was determined by two-tailed Student's $t$ test (Control, $n$ = 4; DLKO, $n$ = 3; *$P$ < 0.05).

# Figure S5 (related to main Figure 5)

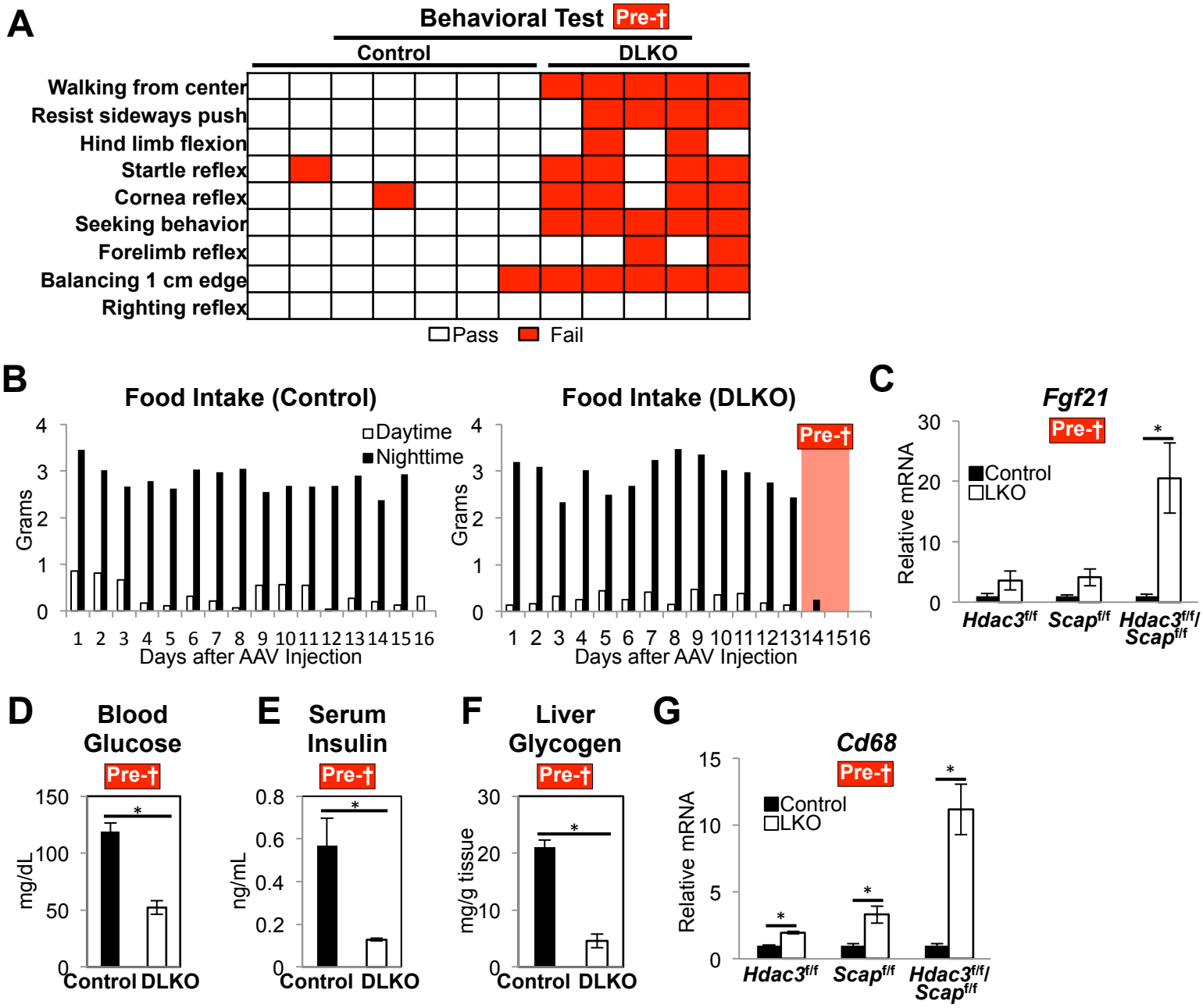


**Figure S5 (related to main Figure 5). Loss of hepatic HDAC3 and SCAP is synthetic lethal.** (**A**) Behavioral test adapted from previous reports (Avraham et al., 2011; Chen et al., 1996) were performed on the moribund cohort (Pre-†; AAV8:Cre) and control mice (AAV8:GFP). (**B**) Representative food intake of control and DLKO mice as measured in real-time by BioDAQ cages. $n = 3$ mice per group. (**C**) RT-qPCR analysis of *Fgf21* expression in livers of moribund (Pre-†) mice. (**D**) Blood glucose measurement of moribund DLKO mice prior to sacrifice. (**E**) Serum insulin levels of moribund DLKO mice. (**F**) Liver glycogen content of moribund DLKO mice. (**G**) RT-qPCR analysis of *Cd68* expression in livers of moribund (Pre-†) mice.
**C** to **G,** n = 4 to 5 mice per group. All error bars, s.e.m. * $P < 0.05$ determined by two-tailed Student's *t* test.

# Figure S6 (related to main Figure 6)

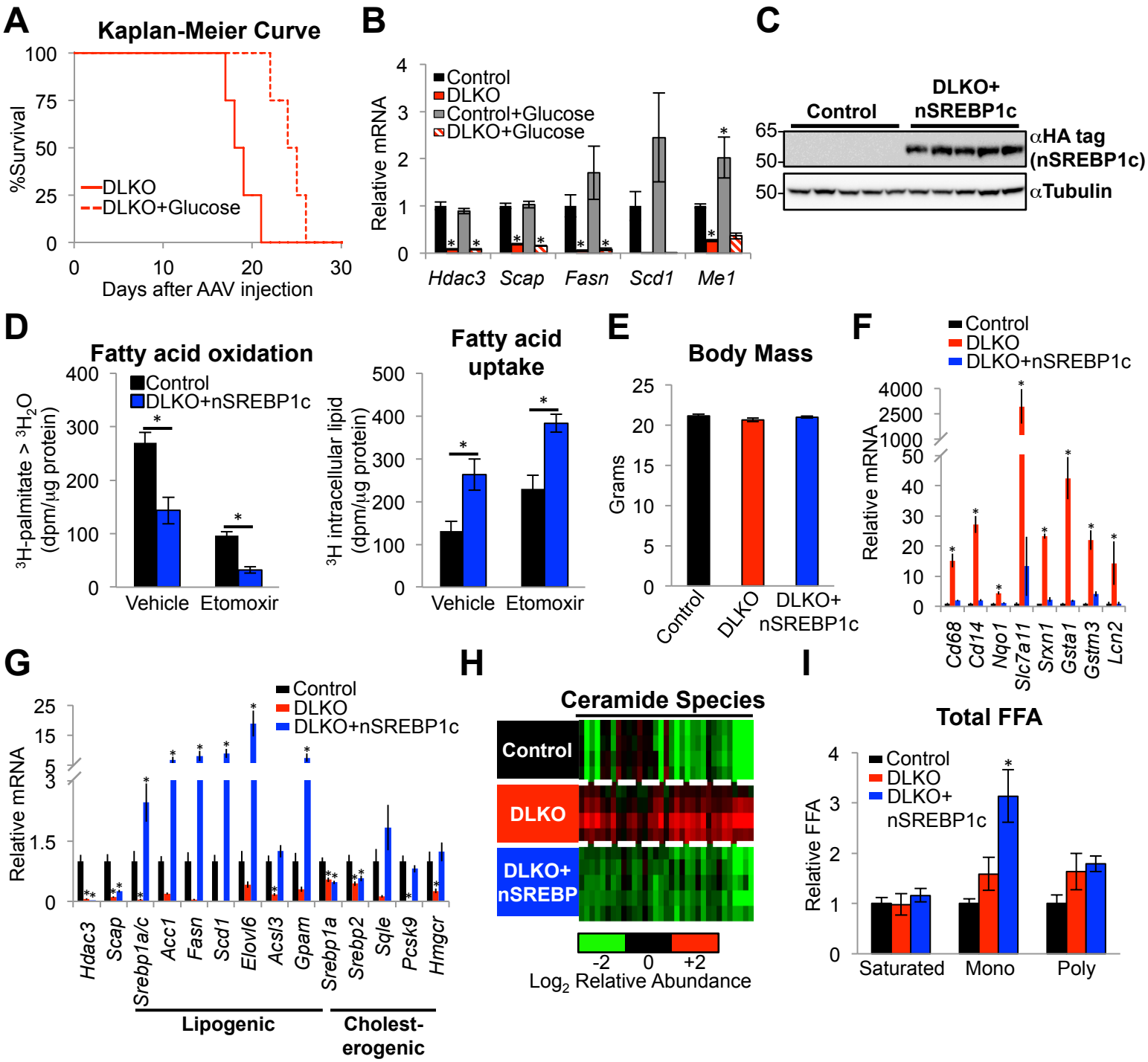


**Figure S6 (related to main Figure 6). Restoration of DNL and TAG synthesis prevents lipotoxicity-induced liver damage.** (**A**) Kaplan-Meier curve of DLKO mice with *ad lib* access to normal chow and 10% glucose supplemented water. *n* = 4 mice per group. (**B**) RT-qPCR analysis of mice from (A) and a DLKO cohort not treated with glucose. *n* = 4 to 6 mice per group. (**C**) Western blot analysis of whole liver extracts. (**D**) Fatty acid oxidation measured in primary hepatocytes. Control cells are from random littermate mice injected with AAV8:GFP. Cells were incubated with $^{3}$H-palmitate for 120 min with vehicle (water) or 100 μM etomoxir (an inhibitor of carnitine palmitoyltransferase-1 and fatty acid oxidation). $^{3}$H-labelled water ($^{3}H_2O$) was measured by scintillation counting. dpm, disintegrations per minute; $^{3}$H-palmiate > $^{3}H_2O$, $^{3}$H-palmitate conversion to $^{3}H_2O$. Fatty acid uptake was measured in the same primary hepatocytes. $^{3}$H-labelled intracellular lipids was extracted and measured by scintillation counting. dpm, disintegrations per minute. *n* = 4 wells (combined from 2 mice) per group. Significance was determined by one-way ANOVA with Tukey's correction (*$P$ < 0.05, comparison between experimental and control cells). (**E,F,G**) Body mass and gene expression analysis of mice sacrificed 12 days post AAV8 injections. *n* = 4 to 5 mice per group. Significance was determined by one-way ANOVA followed by Holm-Sidak correction (*$P$ < 0.05 for comparisons between experimental and control mice). (**H**) Relative abundance of ceramide species. Same cohort as (E). See Table S4 for lipid identification and ion counts. (**I**) Relative changes to saturated, monounsaturated and polyunsaturated FFA species. Significance was determined by one-way ANOVA followed by Tukey's correction (*P < 0.05 for comparisons between experimental and control mice).
All error bars, s.e.m.

# Supplemental Tables and Legends

**Table S1 (Related to Figure 3). Lipidomics analysis of DLKO livers.** Ion counts and statistical analysis are shown in one sheet in this table.

**Table S2 (Related to Figure 3). Lipidomics analysis of HDAC3 LKO and SCAP LKO livers.** Ion counts and statistical analysis are shown in one sheet in this table.

**Table S3 (Related to Figure 4). RNA-seq analysis of LKO livers.** Relative transcript levels in LKO livers ($n$ = 3 - 4) compared to levels in control livers ($n$ = 6). Differentially expressed genes with an FDR <0.1 in at least one condition are shown in one sheet in this table.

**Table S4 (Related to Figure 6). Lipidomics analysis of DLKO and DLKO+nSREBP1c livers.** Ion counts and statistical analysis are shown in one sheet in this table.

**Table S5 (Related to all figures). RT-qPCR primers used throughout the study.**

| Target | Forward | Reverse |
|---|---|---|
| ***Acacb*** | GATGGAGCGCATACACTTGA | CCGAGTTTGTCACTCGGTTT |
| ***Acc1 (Acaca)*** | GATGAACCATCTCCGTTGGC | CCCAATTAT GAATCGGGAGTGC |
| ***Acly*** | AAGAAGGAGGGGAAGCTGAT | TCGCATGTCTGGGTTGTTTA |
| ***Acot2*** | CCCCAAGAGCATAGAAACCA | CCAATTCCAGGTCCTTTTACC |
| ***Acsl3*** | GTCAGGGTCCTGAGGAGGT | CCTCACAGCAAGTTCAAGGA |
| ***Atf4*** | GGGTTCTGTCTTCCACTCCA | AAGCAGCAGAGTCAGGCTTTC |
| ***Atgl*** | TAATGTTGGCACCTGCTTCA | CCACTCACATCTACGGAGCC |
| ***Cd14*** | TTTAACTCTGGCGTAGTCACC | GACCCTCAGAAACCAGGAG |
| ***Cd68*** | GACCTACATCAGAGCCCGAGT | CGCCATGAATGTCCACTG |
| ***Chop*** | CCACCACACCTGAAAGCAGAA | AGGTGAAAGGCAGGGACTCA |
| ***Dgat1*** | ACCTGGCCACAATCATCTG | TGGAGTATGATGCCAGAGCA |
| ***Dgat2*** | GCTGGTGCCCTACTCCAAG | CAGCTTGGGGACAGTGATG |
| ***Edem1*** | CTACCTGCGAAGAGGCCG | GTTCATGAGCTGCCCACTGA |
| ***Elovl5*** | ATGGAACATTTCGATGCGTCA | GTCCCAGCCATACAATGAGTAAG |
| ***Elovl6*** | AATGGATGCAGGAAAACTGG | AACTTGGCTCGCTTGTTCAT |
| ***Fasn*** | TACAGGAGTTCTGGGCCAAC | GACCGCTTGGGTAATCCATA |
| ***Fgf21*** | CTGCTGGGGGTCTACCAAG | CTGCGCCTACCACTGTTCC |
| ***Gpam*** | CAACACCATCCCCGACATC | GTGACCTTCGATTATGCGATCA |
| ***Grp78*** | TTCAGCCAATTATCAGCAAACTCT | TTTTCTGATGTATCCTCTTCACCAGT |
| ***Gsta1*** | CTTCTGACCCCTTTCCCTCT | GCTGCCAGGCTGTAGGAAC |
| ***Gstm1*** | CCCGCATACAGCTCATGATA | TTGCCCAGGAACTCAGAGTAG |
| ***Hdac3*** | CCTGGAACAGGTGACATGTATGA | CGTAAGGGCACATTGAGACAATAG |
| ***Hmgcr*** | GCCCTCAGTTCAAATTCACAG | TTCCACAAGAGCGTCAAGAG |
| ***Insig2*** | CGTGACACTTTTTCCACCAG | GGGTACAACAGCCCAATCAC |
| ***Ire alpha*** | CTCTATGCCTCTCCCTCAATG | ACACTCTCCTTTGTCTCCAATG |
| ***Lcn2*** | CCATCTATGAGCTACAAGAGAACAAT | TCTGATCCAGTAGCGACAGC |
| ***Lipa*** | AGTATTCACCGAATCCCTCG | CTAGAATCTGCCAGCAAGCC |
| ***Me1*** | GGGATTGCTCACTTGGTTGT | GTTCATGGGCAAACACCTCT |
| ***Nqo1*** | AGCGTTCGGTATTACGATCC | AGTACAATCAGGGCTCTTCTCG |
| ***Pcsk9*** | TTTTATGACCTCTTCCCTGGC | ATTCGCTCCAGGTTCCATG |
| ***Scap*** | CTGTGAAGGGTTACTCGCC | AAGATTTCTGTGCCAGGGAG |
| ***Scd1*** | GCTCTACACCTGCCTCTTCG | GCCGTGCCTTGTAAGTTCTG |
| ***Slc7a11*** | GATTCATGTCCACAAGCACAC | AGAGCATCACCATCGTCAGA |
| ***Sqle*** | CCCCAAAACACAAAATCCTCAG | GCAATGCCAAGAAAAGTCCAC |
| ***Srebp1a*** | CCGAGATGTGCGAACTGG | GGGAAGTCACTGTCTTGGTTG |
| ***Srebp1a/c*** | CCATCGACTACATCCGCTTC | GCCCTCCATAGACACATCTG |
| ***Srebp2*** | CCCTATTCCATTGACTCTGAGC | CACATAAGAGGATTCGAGAGCG |
| ***Srxn1*** | AGGGGCTTCTGCAAACCTA | TGGCATAGCTACCTCACTGCT |
| ***Tgm2*** | CCTGACCCTGGATCCCTACT | CACCCGCTGTACTTCTCGTAG |
| ***Xbp1t (total)*** | TGGCCGGGTCTGCTGAGTCCG | GTCCATGGGAAGATGTTCTGG |
| ***Xbps (spliced)*** | CTGAGTCCGAATCAGGTGCAG | GTCCAT GGGAAGATGTTCTGG |

# Supplemental Experimental Procedures

**Western blot and gene expression analysis.** Antibodies used in western blots include: anti-HDAC3 (1:2000, ab7030, Abcam), anti-SCAP (1:100, sc-9675, Santa Cruz Biotechnology), anti-SREBP1 (1:500, sc-13551x, Santa Cruz Biotechnology), anti-Actin (1:2000, #4967, Cell Signaling Technology), anti-phospho NF-κB (S536) (1:1000, #3033, Cell Signaling Technology), anti-phospho JNK (T183/Y185) (1:500, #9251, Cell Signaling Technology), anti-NF-κB (1:1000, #4764, Cell Signaling Technology), anti-JNK2 (1:1000, #9258, Cell Signaling Technology), anti-Tubulin[HRP] (1:2000, ab21058, Abcam), and anti-HA tag[HRP] (1:1000, #2999, Cell Signaling Technology). HRP-conjugated anti-rabbit and anti-mouse secondary antibodies (GE Amersham) were used at a dilution of 1:5000. Western blot signals were detected by SuperSignal West Dura Extended Duration Substrate (ThermoFisher Scientific) and imaged with a BioRAD ChemiDoc Touch imaging system. Band quantification was done with Image Lab software. For reverse transcriptase quantitative PCR (RT-qPCR), total RNA from livers was extracted with TRIzol reagent (ThermoFisher Scientific), treated with Dnase and purified with RNeasy Kit (Qiagen). Following cDNA generation with High-Capacity cDNA RT kit (Applied Biosystems), RT-qPCR was performed with a SYBR Green PCR master mix and a QuantStudio 6 Flex instrument (Applied Biosystems) using a standard curve analysis. See Table S5 for primer sequences. RNA sequencing libraries were prepared from 1 μg total RNA using the TruSeq RNA Sample Preparation Kit v2 (Illumina) according to manufacturer's protocol. Differentially expressed genes in Control, HDAC3 LKO, SCAP LKO and DLKO livers were identified by edgeR bioconductor package. Processed RNA-seq data is available in Table S3.

**ChIP sequencing and analysis.** ChIPed DNA was amplified according to ChIP sequencing sample preparation guide provided by Illumina, using adaptor oligo primers from Illumina, enzymes from New England Biolabs and PCR purification kits from Qiagen. Biological replicates were barcoded and sequenced. Deep sequencing was performed by the functional Genomics Core (J. Schug) of the Penn Diabetes Endocrinology Research Center using Illumina HiSeq2000.

*Sequencing data processing*. Sequencing reads were aligned to the mm9 genome using Bowtie v1 (Langmead et al., 2009). PCR duplicates were removed and peaks were called on individual replicates using HOMER v4.6 (Heinz et al., 2010). Peaks below 4-fold cutoff over input (HA ChIP in AAV8:GFP mice or HDAC3 ChIP in HDAC3 LKO mice) were removed. High-confidence peaks were found by using a 2 rpm cutoff in 2 out of 2 replicates (HA ChIPs) or 2 out 3 replicates (HDAC3 ChIPs) for each condition. Peaks were merged using HOMER's mergePeaks command, using at least 50% overlap. Heat maps, average profiles and motifs were generated using HOMER and R (R Development Core Team, 2008).

**Metabolomics.** For water-soluble metabolites, the pulverized tissue powder was mixed by vortexing with 1 mL of -80°C 80:20 methanol:water, and placed on dry ice for 10 min. Samples were centrifuged at >15,000 RCF for 10 min and the supernatants collected as the first extract. The insoluble material was extracted one more time with 1 mL of -80°C 80:20 methanol:water. The supernatants from two rounds of extraction were combined, dried under nitrogen flow, and re-dissolved in LC-MS grade water using a ratio of 1 mL of water per 25 mg initial tissue weight and analyzed on two separate instrument platforms to cover both positive charged and negative charged metabolites. Negative charged metabolites were analyzed via reverse-phase ion-pairing chromatography coupled to an Exactive orbitrap mass spectrometer (ThermoFisher Scientific, San Jose, CA). The mass spectrometer was operated in negative ion mode with resolving power of 100,000 at m/z 200, scanning range being *m/z* 75-1000. The LC method has been described before(Lu et al., 2010), using a Synergy Hydro-RP column (100 mm × 2 mm, 2.5 μm particle size, Phenomenex, Torrance, CA) with a flow rate of 200 μL/min. The LC gradient was 0 min, 0% B; 2.5 min, 0% B; 5 min, 20% B; 7.5 min, 20% B; 13 min, 55% B; 15.5 min, 95% B; 18.5 min, 95% B; 19 min, 0% B; 25 min, 0% B. Solvent A is 97:3 water:methanol with 10 mM tributylamine and 15 mM acetic acid; solvent B is methanol. Positive charged metabolites were analyzed on a Q Exactive Plus mass spectrometer coupled to Vanquish UHPLC system (ThermoFisher Scientific, San Jose, CA). The mass spectrometer was operated in positive ion mode with resolving power of 140,000 at m/z 200, scanning range being m/z 75-1000. The LC separation was achieved on an Agilent Poroshell 120 Bonus-RP column (150 x 2.1 mm, 2.7 μm particle size). The gradient was 0 min, 50 μL/min, 0.0%B; 6 min, 50 μL/min, 0% B; 12 min, 200 μL/min, 70% B; 14 min, 200 μL/min, 100 %B; 18 min, 200 μL/min, 100% B; 19 min, 200 μL/min, 0% B;

24 min, 200 µL/min, 0% B; 25 min, 50 µL/min, 0% B. Solvent A is 10mM ammonium acetate + 0.1% acetic acid in 98:2 water:acetonitrile and solvent B is acetonitrile.

For fatty acids and lipids, pulverized tissue powder was mixed by vortexing with 1 mL of 0.1 M HCl in 50:50 methanol:H2O and sit in -20°C freezer for 30 min. Then 0.5 mL of chloroform was added to the mixture and vortex to mix well, and let it sit on ice for 10 min. Samples were centrifuged at >15,000 RCF for 10 min and the chloroform phase at bottom was transferred to a glass vial as the first extract using a Hamilton syringe. 0.5 mL chloroform was added to the remaining material and the extraction was repeated to get the second extract. The combined extract was dried under nitrogen flow and re-dissolved in solvent of 1:1:1 methanol:chloroform:2-propanol using a ratio of 1 mL of solvent per 25 mg of initial tissue weight. Fatty acids and lipids were analyzed on a Q Exactive Plus mass spectrometer coupled to vanquish UHPLC system (ThermoFisher Scientific, San Jose, CA). Each sample was analyzed twice using same LC gradient but different ionization mode on mass spectrometer to cover both positive charged and negative charged species. The LC separation was achieved on an Agilent Poroshell 120 EC-C18 column (150 x 2.1 mm, 2.7 µm particle size) at a flow rate of 150 µL/min. The gradient was 0 min, 25% B; 2 min, 25% B; 4 min, 65% B; 16 min, 100 %B; 20 min, 100% B; 21 min, 25% B; 27 min, 25% B. Solvent A is 1mM Ammonium acetate + 0.2% acetic acid in water:methanol (90:10). Solvent B is 1mM Ammonium acetate + 0.2% acetic acid in Methanol:2-propanol (2:98).

Data analyses were performed using MAVEN software, which allows for sample alignment, feature extraction and peak picking (Melamud et al., 2010). Exacted ion chromatogram for each metabolite was manually examined to obtain its signal, using a custom made metabolite library.

**Flow cytometry.** We collected the left major lobe from each mouse. Each piece was digested with collagenase, homogenized, purified of red blood cells by lysis, and stained at a 1:200-400 dilution with mouse fluorochrome-conjugated monoclonal antibodies specific for CD3ε (17A2), CD11b (M1/70), CD19 (6D5), CD45 (30-F11), CD68 (FA-11), Ly6g (1A8), and Siglec F (E50-2440) (BioLegend, BD Pharmingen). We acquired cells with a LSR II with DiVa software (BD Bioscience) and analyzed data with FlowJo software (Tree Star).

# Supplemental References


Avraham, Y., Grigoriadis, N.C., Poutahidis, T., Vorobiev, L., Magen, I., Ilan, Y., Mechoulam, R., and Berry, E.M. (2011). Cannabidiol improves brain and liver function in a fulminant hepatic failure-induced model of hepatic encephalopathy in mice. Br. J. Pharmacol. *162*, 1650–1658.

Chen, Y., Constantini, S., Trembovler, V., Weinstock, M., and Shohami, E. (1996). An experimental model of closed head injury in mice: pathophysiology, histopathology, and cognitive deficits. J. Neurotrauma *13*, 557–568.

Heinz, S., Benner, C., Spann, N., Bertolino, E., Lin, Y.C., Laslo, P., Cheng, J.X., Murre, C., Singh, H., and Glass, C.K. (2010). Simple Combinations of Lineage-Determining Transcription Factors Prime cis-Regulatory Elements Required for Macrophage and B Cell Identities. Mol. Cell *38*, 576–589.

Langmead, B., Trapnell, C., Pop, M., and Salzberg, S.L. (2009). Ultrafast and memory-efficient alignment of short DNA sequences to the human genome. Genome Biol. *10*, R25.

Lu, W., Clasquin, M.F., Melamud, E., Amador-Noguez, D., Caudy, A.A., and Rabinowitz, J.D. (2010). Metabolomic analysis via reversed-phase ion-pairing liquid chromatography coupled to a stand alone orbitrap mass spectrometer. Anal. Chem. *82*, 3212–3221.

Melamud, E., Vastag, L., and Rabinowitz, J.D. (2010). Metabolomic analysis and visualization engine for LC-MS data. Anal. Chem. *82*, 9818–9826.

R Development Core Team (2008). R: A Language and Environment for Statistical Computing. Vienna Austria R Found. Stat. Comput. *1*, 2673.